Journal of Physics: Conference Series **447** (2013) 012044 doi:10.1088/1742-6596/447/1/012044

Higgs Boson Searches at ATLAS

R. Gonçalo on behalf of the ATLAS Collaboration
Royal Holloway, University of London
E-mail: jose.goncalo@cern.ch

Abstract. The present article gives an overview of the status of Higgs boson studies in the ATLAS experiment at the LHC, at the time of the DISCRETE 2012 Symposium. Accounts of the latest Higgs boson searches in the $H \to WW^{(*)} \to \ell\nu\ell\nu$, $H \to b\bar{b}$ and $H \to \tau^+\tau^-$ channels are given, as well as a summary of the investigation into the couplings of the new particle, and an indication of the sensitivity of future Higgs studies at the LHC.

1. Introduction

The discovery [1, 2] of a new particle in the search for the Standard Model Higgs boson at the LHC represents a major milestone in the understanding of the mechanism responsible for electroweak symmetry breaking. After this discovery, it is now crucial to establish if the new particle is indeed the Higgs boson predicted by the Standard Model (SM) or whether it could provide evidence for physics beyond the SM. To do that, it is essential to make clear observations of the new particle in all expected channels and measure its properties accurately.

The new particle discovery in ATLAS [3] was based on datasets with integrated luminosities of 4.8 fb^{-1} and 5.8 fb^{-1}, produced at centre of mass energies of $\sqrt{s} = 7$ TeV and $\sqrt{s} = 8$ TeV, respectively [1]. At the LHC, the Higgs boson is produced predominantly through a top quark dominated loop in the gluon-fusion process (ggF). Vector boson fusion (VBF), comes next in cross section, where the Higgs is produced by the fusion of two W or Z bosons, followed by the associated production of the Higgs boson with a single W or Z (VH), or with a pair of top quarks ($t\bar{t}H$). Five decay channels were combined in the discovery of the new particle: $H \to ZZ^{(*)} \to 4\ell$, $H \to \gamma\gamma$, $H \to WW^{(*)} \to \ell\nu\ell\nu$, $H \to \tau^+\tau^-$, and $H \to b\bar{b}$ [1].

Clear observations of the new particle in a single channel have so far been made in analyses focusing on bosonic decays, such as $H \to ZZ^{(*)} \to 4\ell$ and $H \to \gamma\gamma$. Fermionic decay channels such as $H \to \tau^+\tau^-$ and $H \to b\bar{b}$ will play an important role in ascertaining the nature of the new particle. Our present knowledge of the new particle indicates that it is a neutral resonance with a mass in the region of 125 GeV (as observed in the $H \to \gamma\gamma$ and $H \to ZZ^{(*)} \to 4\ell$ channels). The observation in the $H \to \gamma\gamma$ channel disfavours a spin 1 particle [4].

Our knowledge of the coupling properties of the new particle is discussed in section 2. This is followed by updates of the $H \to WW^{(*)} \to \ell\nu\ell\nu$, $H \to \tau^+\tau^-$ and $H \to b\bar{b}$ ATLAS searches, in sections 3, 4, and 5. Finally, section 6 gives an impression of what results can be expected from ATLAS given 300 fb^{-1} and 3000 fb^{-1}of $\sqrt{s} = 14$ TeV collision data.

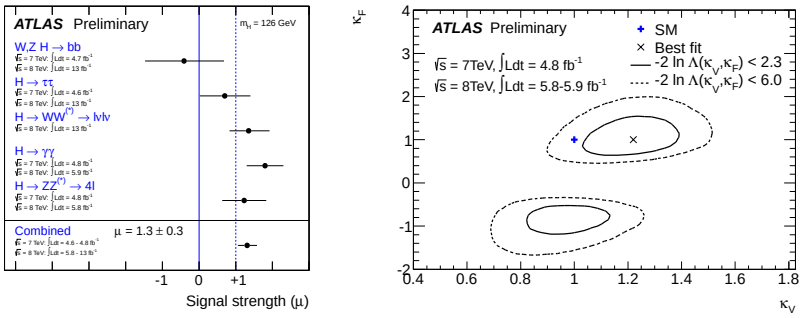

Figure 1. Left: signal strength parameter μ for $m_H = 126$ GeV for the individual channels and their combination [8]. Right: 68% and 95% CL contours for the fit to the fermion (κ_F) and vector (κ_V) coupling scale factors [5].

2. Coupling properties of the new particle

The same data, analyses, and statistical models used for the ATLAS discovery was examined to investigate the couplings of the new particle [5]. It is convenient to define a *signal strength* observable, μ, as the ratio of the observed cross section to the SM expected cross section, $\mu = \sigma/\sigma_{SM}$, in each investigated channel or the statistical combination of several channels. The background-only hypothesis corresponds to $\mu = 0$ and the SM hypothesis including the Higgs boson corresponds to $\mu = 1$. The couplings of the new particle are investigated with the following assumptions [6]: only modifications of coupling strengths are taken into account; the new particle is assumed to be a single, CP-even scalar, as expected of the SM Higgs boson; it is assumed to have a mass of 126 GeV with a negligible width. This allows the product of the cross section and branching ratio in each channel $ii \to H \to ff$ to be decomposed as: $\sigma \times BR = \sigma_{SM}(ii \to H) \times BR_{SM}(H \to ff) \times \frac{\kappa_i^2 \kappa_f^2}{\kappa_H^2}$ where the κ factors multiply the Yukawa couplings of each initial- (i) or final-state (f) particle flavour.

This is a convenient and flexible framework in which to explore the couplings of the new particle. It should be noted, however, that new physics responsible for a deviation of the observed couplings with respect to the SM ones might also modify the kinematics of particles in the observed final states. This is not accounted for by this framework, which is however still assumed to be valid to identify small deviations in the observed couplings with respect to the SM expectations. The fit to the experimental data is done using a profile likelihood method [7].

The simplest model tested in this framework assumes all coupling parameters are modified by a single scaling factor κ, which corresponds to the square root of the global signal strength $\mu = 1.4 \pm 0.3$ [5]. The fit to the data yields $\kappa = 1.19 \pm 0.11(stat) \pm 0.03(syst) \pm 0.06(theory)$. The combined signal strength value has since been updated [8] and is shown in Figure 1 (left).

A different benchmark scenario can be explored by assuming a single scale factor $\kappa_F = \kappa_t = \kappa_b = \kappa_\tau$ for all fermion couplings, and a different one, $\kappa_V = \kappa_W = \kappa_Z$, for vector bosons. In addition to the weak constraints provided by the $H \to b\bar{b}$ and $H \to \tau^+\tau^-$ channels, sensitivity to the fermion coupling comes from the top-quark loop in the gluon-fusion diagram contributing to several channels. Sensitivity to the vector boson coupling parameter is provided by $H \to \gamma\gamma$, $H \to ZZ^{(*)} \to 4\ell$, and $H \to WW^{(*)} \to \ell\nu\ell\nu$ decays. Assuming further that only SM particles contribute to the Higgs boson width, a fit to the coupling strength scale factors can be made. Figure 1 (right) shows the correlation between κ_F and κ_V scale factors. Only the relative sign between κ_F and κ_V is physical, so negative values of the scale factors are shown. Some sensitivity to this sign is found from the negative interference between the W and t loops in $H \to \gamma\gamma$ decays.

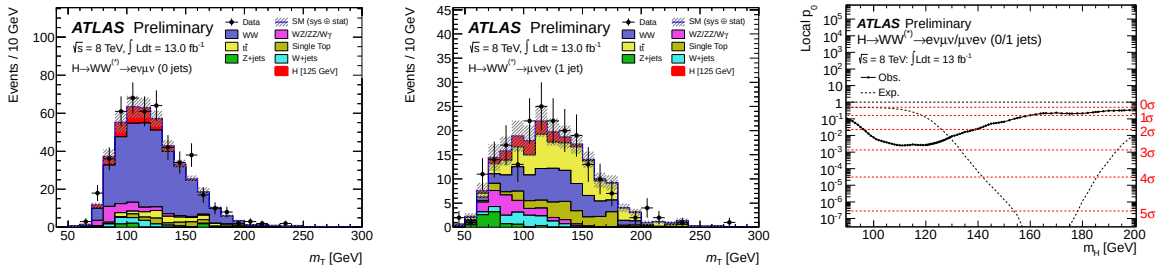

Figure 2. Transverse mass distribution in the $H+0$-jet category of the $H \to WW^{(*)} \to \ell\nu\ell\nu$ analysis (left) and the $H+1$-jet category (centre) [9]. Right: probability for the background-only hypothesis, p_0, for $H \to WW^{(*)} \to \ell\nu\ell\nu$ combining all analysis categories [9]. The solid line corresponds to the observed p_0, while the dashed line corresponds to the expectation for the signal+background hypothesis as a function of the mass of the hypothesised signal.

The fit shows a small preference for the local minimum near the SM expectation.

3. $H \to WW^{(*)} \to e\nu\mu\nu$ search with $\sqrt{s} = 8$ TeV LHC data

The latest ATLAS $H \to WW^{(*)} \to \ell\nu\ell\nu$ search [9] uses 13 fb^{-1} of $\sqrt{s} = 8$ TeV pp data and updates the previously published results [1]. The high branching ratio of this channel ($BR(H \to WW^{(*)} \to \ell\nu\ell\nu) \approx 22\%$ for m_H around 125 GeV [10]) and the availability of leptonic final states which facilitate triggering and rejecting the main backgrounds make this a very sensitive channel. The updated analysis focuses on the $H \to WW^{(*)} \to e\nu\mu\nu$ channel. In addition to two isolated, opposite charge leptons of different flavour and high transverse momentum (p_T above 15 or 25 GeV), events are required to have a large missing transverse momentum (E_T^{miss}) relative to the direction of the direction of the leading lepton or the closest jet, $E_{T,rel}^{miss}$. Due to spin correlations in the $WW^{(*)}$ system, arising from the spin-0 nature of the SM Higgs boson and the V-A structure of W boson decay, the charged leptons tend to have similar directions for the SM Higgs signal and a flatter distribution for the dominant WW background. This feature is exploited by requiring the di-lepton invariant mass, $m_{\ell\ell}$ to be less than 50 GeV, and the azimuthal angle difference between the two leptons, $\Delta\phi_{\ell\ell}$ less than 1.8 radians.

The background composition depends on the jet multiplicity. Events are therefore classified into $H+0$-jet and $H+1$-jet categories, and different cuts are applied to improve the sensitivity in each one. In this and the following analyses, jets are reconstructed using the anti-k_t algorithm [11] with distance parameter R=0.4. Events with higher jet multiplicity are dominated by top quark production and are not considered in the statistical analysis. An important feature of this and later analyses is the data-driven determination of the most important sources of background with the help of control regions enriched in each process. The main backgrounds are WW and top production (both $t\bar{t}$ and single-top), but W+jets and $Z/\gamma^* \to \tau\tau$ are also determined from specific control samples. More details can be found in [9].

The presence of high transverse momentum neutrinos in the signal prevents the reconstruction of the Higgs boson mass. A transverse mass variable, m_T [9], is thus used as the final discriminating variable in the statistical analysis. Figure 2 (left and middle) shows distributions of this variable in the $H+0$-jet and $H+1$-jet categories. The statistical analysis of the m_T distribution in each category employs a binned likelihood, $\mathcal{L}(\mu, \theta)$, constructed as the product of Poisson probability terms. This depends on the signal strength, μ, and on a set of nuisance parameters, θ, which affect signal and background predictions [7]. The probability

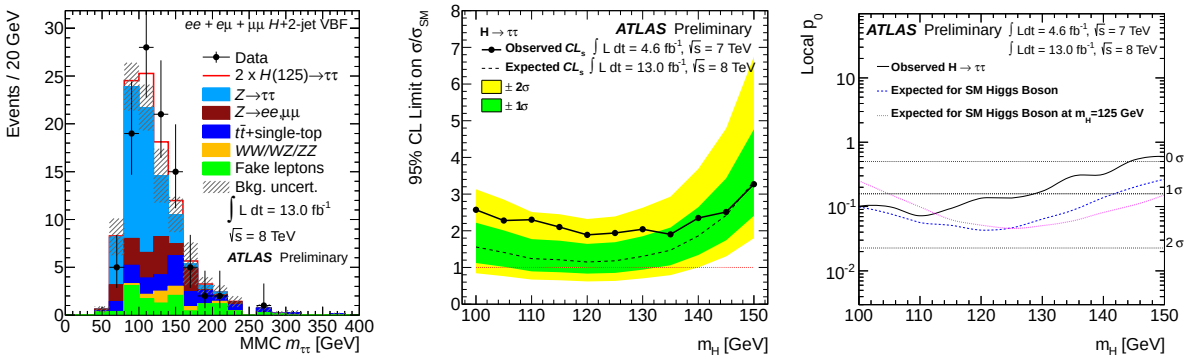

Figure 3. Left [12]: reconstructed $m_{\tau\tau}$ for events selected into the *VBF* category of the $H \to \tau_{lep}\tau_{lep}$ channel. Centre [12]: observed (solid) and expected (dashed) 95% CL limits on the Higgs boson cross section as a function of the Higgs boson mass, normalized to the SM cross section, combining all categories in the $H \to \tau_{lep}\tau_{lep}$, $H \to \tau_{lep}\tau_{had}$, and $H \to \tau_{had}\tau_{had}$ channels. Right [12]: observed (solid) and expected (dashed) local p_0 as a function of the Higgs boson mass. The dotted line corresponds to the expected p_0 curve calculated for the 125 GeV SM Higgs mass hypothesis as a function of the reconstructed Higgs boson mass. The broad minimum in this curve is caused by the poor resolution of the reconstructed $m_{\tau\tau}$.

of the background-only hypothesis, p_0, is calculated in the statistical analysis, as well as the exclusion limits on the signal cross section, following the CL_s method [13]. Figure 2 (right) shows the p_0 value observed in the $H \to WW^{(*)} \to \ell\nu\ell\nu$ search, combining the various analysis categories. A broad minimum is observed, which is caused by the poor mass resolution of the m_T discriminating variable. The observed p_0 value for $m_H = 125$ GeV is 4×10^{-3}, corresponding to 2.6 standard deviations from the background-only hypothesis.

4. $H \to \tau\bar{\tau}$ searches

Due to the relatively high mass of tau leptons, the $H \to \tau^+\tau^-$ decay corresponds to the dominant leptonic decay mode of the SM Higgs boson ($BR(H \to \tau^+\tau^-) \approx 6.3\%$). Both leptonic ($\tau_{lep}$) and hadronic ($\tau_{had}$) decays of the tau lepton were considered in this search [12], which considered the $H \to \tau_{lep}\tau_{lep}$, $H \to \tau_{lep}\tau_{had}$, and $H \to \tau_{had}\tau_{had}$ decay channels. Events were selected by requiring exactly two opposite-charge reconstructed τ candidates. The invariant mass of the $\tau^+\tau^-$ system, $m_{\tau\tau}$, was used as the discriminant variable in all three analyses, and was estimated with a $m_{\tau\tau}$ resolution of 13 – 20% [14], depending on the event topology and kinematics. Events were further subdivided into different categories to target different topologies, the main ones being the *VBF* category, containing events with two high-p_T jets widely separated in rapidity, and the *Boosted* category, which includes events with a high transverse momentum of the $\tau\tau$ system. Other less significant categories were considered, and more details can be found in [12].

As can be seen in Figure 3 (left), the main source of background after the event selection is $Z \to \tau\tau$, with other sources such as top (both $t\bar{t}$ and single top), multijet production, and backgrounds from τ mis-identification being important in some categories. To avoid uncertainties in the simulation of $Z \to \tau\tau$ production, this background was modelled by selecting a sample of $Z \to \mu\mu$ in collision data and replacing the muon momenta with simulated tau leptons decays. Other backgrounds were estimated from collision data in control samples defined by inverting selection cuts specific to each analysis category. A detailed account can be found in [12].

Figure 3 (centre) shows the 95% confidence level (CL) exclusion limits on the signal strength, as a function of the Higgs boson mass, estimated for the combined $H \to \tau^+\tau^-$ analysis categories.

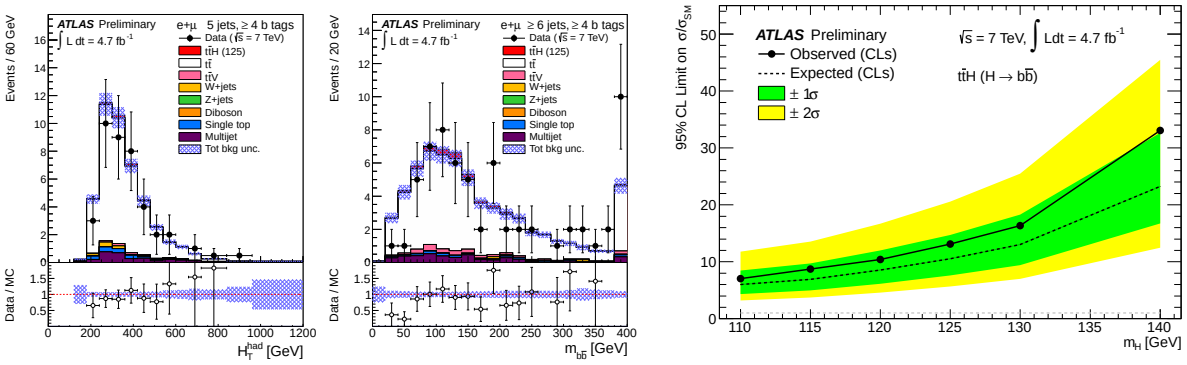

Figure 4. Examples of the final discriminant variables used in the analysis categories with 5 jets, ≥ 4 of which are b-tagged (left, $H_T^{\rm had}$) and ≥ 6 jets, ≥ 4 of which are b-tagged (right, $m_{b\bar{b}}$), after the statistical analysis which constrains various sources of systematic uncertainty [15]. Right: observed and expected 95% CL upper limits [15] on $\sigma(t\bar{t}H) \times BR(H \to b\bar{b})$ relative to the SM prediction, as function of m_H.

A broad excess of the observed limit with respect to the expected limit, could indicate the presence of signal. The local p_0 value for this channel is shown in Figure 3 (right) and shows that this excess corresponds at most to a 1.5σ deviation from the background-only hypothesis.

5. $H \to b\bar{b}$ searches

The Higgs boson decays predominantly to a pair of b quarks in the mass region of $m_H \approx 125$ GeV ($BR(H \to b\bar{b}) \simeq 58\%$ [10]). On the other hand, the experimental observation of the dominant ggF production mechanism is extremely challenging, due to the overwhelming background from multijet production. Instead, the ATLAS searches concentrate on channels where the Higgs boson is produced in association with gauge bosons, WH and ZH, or top quarks, $t\bar{t}H$. These analyses relied on a b-tagging algorithm tuned to identify true b-initiated jets with an efficiency of 70%, and rejection factors of around 5 and 150 for c-quark jets and light-quark jets, respectively.

5.1. $H \to b\bar{b}$ searches in associated production channels with a top quark pair

As the SM Higgs coupling to fermions is proportional to the fermion mass, the $t\bar{t}H$ channel provides experimental sensitivity to the largest Higgs coupling constant. It is also free from assumptions that affect other channels sensitive to this coupling through loops. A search [15] the $t\bar{t}H \to b\bar{b}\ b\ell\nu\ bqq$ decay channel was performed using 4.7 fb^{-1} of $\sqrt{s} = 7$ TeV LHC data. Events were required to have an electron (muon) with p_T above 25 GeV ($p_T > 20$ GeV) and at least four jets with p_T above 25 GeV. Additional cuts were applied on E_T^{miss} and m_T [15]. Selected events were classified into different categories depending on the jet multiplicity and on how many jets were b-tagged. The signal to background ratio is highest for events containing at least 5 jets, 3 of which are b-tagged. For each category, a discriminating variable was considered: either the scalar sum of jet transverse momenta ($H_T^{\rm had}$) or the invariant mass of the two jets most likely to originate from the Higgs boson decay ($m_{b\bar{b}}$). In the analysis categories where $m_{b\bar{b}}$ is used (with 6 jets and 3 or ≥ 4 jets), a kinematic likelihood fit was performed to reconstruct the $t\bar{t}$ system in each event. The remaining b-tagged jets were identified as Higgs boson decay products.

In addition to improving the analysis sensitivity, the analysis categories were used in the statistical analysis to constrain nuisance parameters corresponding to various sources of

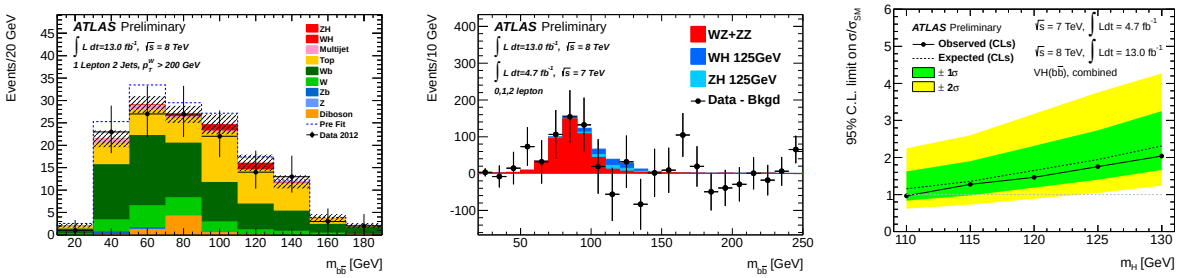

Figure 5. Left [16]: $m_{b\bar{b}}$ distribution in data and simulation for the 1-lepton channel in the analysis category with $p_T^V > 200$ GeV category. The background expectation is shown before (dashed line) and after the statistical analysis which constrains the normalisation of several sources of background. Centre [16]: $m_{b\bar{b}}$ distribution in after subtraction of all backgrounds except diboson processes, including SM Higgs boson from WH and ZH associated production. Right [16]: expected (dashed) and observed (solid) 95% CL upper limit on σ/σ_{SM} relative to the SM prediction, as function of m_H.

background and of systematic uncertainty. Categories with 4 jets and ≥ 2 b-tagged jets are dominated by $t\bar{t}$ production. The distribution of this background across the 0, 1, and ≥ 2 b-tag categories provides a powerful constraint on the b-tagging efficiency systematic uncertainty. Categories with 4, 5 and ≥ 6 jets and ≥ 2 b-tagged jets constrain the $t\bar{t}$ model uncertainties, which may result in large distortions of the shape of the $H_T^{\rm had}$ variable. Figure 4 (left and centre) shows distributions of the discriminating variables, $H_T^{\rm had}$ and $m_{b\bar{b}}$, where the uncertainties are constrained by the statistical analysis fit to the data. This is reflected in the small uncertainty bands of the expected distributions. The limits on the Higgs boson signal strength (σ/σ_{SM}) are shown in Figure 4 (right) as a function of the Higgs boson mass. For a mass of 125 GeV, an exclusion limit of $13.1 \times \sigma_{SM}$ ($10.5 \times \sigma_{SM}$) was observed (expected) at the 95% CL.

5.2. $H \to b\bar{b}$ searches in associated VH production

The ATLAS search [16] for associated production of the Higgs boson with a W or a Z vector boson (VH) was made in three exclusive channels, corresponding to events containing 0, 1, or 2 charged leptons, in addition to two b-tagged jets. These target respectively the $ZH \to \nu\bar{\nu}b\bar{b}$ $WH \to \ell\nu b\bar{b}$ and $ZH \to \ell\ell b\bar{b}$ decay channels, where ℓ refers to an electron or a muon. It used 4.7 fb^{-1} of $\sqrt{s} = 7$ TeV LHC data and 13.0 fb^{-1} of $\sqrt{s} = 8$ TeV data. This analysis updated a previously published analysis [17] by re-optimizing selection cuts and the analysis strategy.

In the 0-lepton channel, transverse energy triggers were used, with efficiencies above 50% for E_T^{miss} above 120 GeV, and essentially 100% for E_T^{miss} above 160 GeV. The trigger turn-on curve in simulated events was corrected to that obtained in data using W+jets events. In all categories, jets were selected with cuts of $p_T > 45$ GeV and $p_T > 25$ GeV for the leading and remaining jets, respectively. The main background in the 2-lepton channel is Z+jets production, whereas both top (single-top and $t\bar{t}$) and W+jets are the main backgrounds affecting the 1-lepton analysis (see Figure 5). All three backgrounds are significant in the 0-lepton analysis. Cuts are applied to topological variables which were optimized for each channel and event category. In each channel, events were further classified into separate categories defined by the transverse momentum of the reconstructed vector boson, p_T^V. The p_T^V categories in the 1- and 2-lepton analyses were: $p_T^V \in [0, 50], [50, 100], [100, 150], [150, 200]$ or ≥ 200 GeV. For the 0-lepton channel, $p_T^V = E_T^{miss}$ was assumed, and the categories were: $E_T^{miss} \in [120, 160], [160, 200]$ or > 200 GeV, separated further into 2-jet and 3-jet categories. The higher-p_T^V categories show an increasing ratio of signal

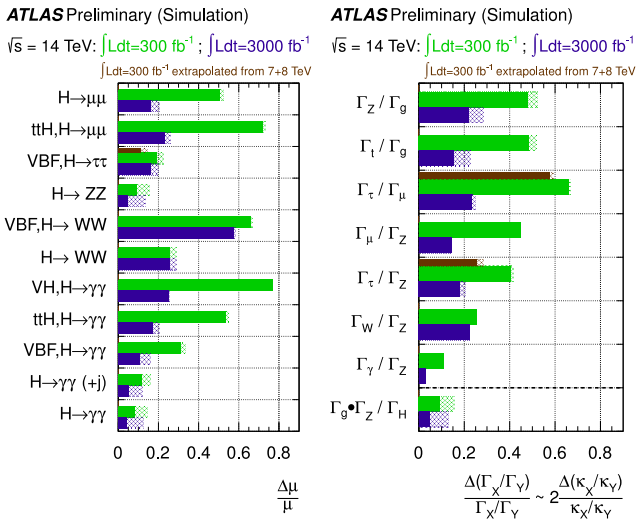

Figure 6. Left [18]: expected relative uncertainty on the signal strength μ in various Higgs boson analyses, assuming a Higgs mass of 125 GeV, for integrated luminosities of 300 fb^{-1} and 3000 fb^{-1} of pp LHC data at $\sqrt{s} = 14$ TeV. Right [18]: expected relative uncertainty on ratios of Higgs boson partial widths. No assumptions were made on the total Higgs boson width, and so on the presence of new physics. For the $H \to \tau^+\tau^-$ channel, the thin brown bars correspond to the extrapolation of the analyses performed using the current data to higher luminosities.

to background, and drive the analysis sensitivity. Control samples rich in top events were also used in the statistical analysis. The invariant mass of the $b\bar{b}$ system, $m_{b\bar{b}}$, was the discriminating variable used in all categories. As in the previous analysis, the main sources of background, top, $W + b$ jets, and $Z + b$ jets, were constrained from the data during the statistical analysis.

The production of WZ and ZZ with one Z boson decaying as $Z \to b\bar{b}$ has a very similar signature as the VH signal, but with a cross section $\approx$ 5 times higher, and p_T^V amd $m_{b\bar{b}}$ distributions peaking at lower values. As a validation of the VH search, a separate fit was made by fixing the Higgs cross section at its SM value and fitting the amount of diboson background. Figure 5 (centre) shows the resulting $m_{b\bar{b}}$ distribution after subtracting all sources of background except for the diboson contribution. The measured diboson signal strength is $\mu_D = 1.09 \pm 0.20(stat) \pm 0.22(syst)$, in agreement with the SM expectation, and corresponded to a significance of 4.0 σ. After fixing the diboson contribution to its SM value, a fit was performed to the Higgs boson signal strength to extract the 95% CL exclusion limits. Figure 5 (right) shows the result of this fit for the combination of all channels and analysis categories as a function of the Higgs boson mass. For a mass of $m_H = 125$ GeV, a 95% CL exclusion limit of $1.8 \times \sigma_{SM}$ $(1.9 \times \sigma_{SM})$ was observed (expected).

6. The long view

The first long period of LHC running has finished with around 25 fb^{-1} of pp collision data collected by ATLAS at $\sqrt{s} = 7$ TeV and $\sqrt{s} = 8$ TeV. The currently foreseen experimental program should provide $\approx$ 300 fb^{-1} of pp data at $\sqrt{s} = 13 - 14$ TeV by 2021. At this point the LHC luminosity may be further enhanced to provide a total integrated luminosity of around 3000 fb^{-1}. A study of the achievable sensitivity of Higgs boson studies was performed in ATLAS taking into account these luminosity scenarios [18]. The estimated performance of the ATLAS detector and reconstruction algorithms was taken into account in an approximate

way. In addition to existing analyses of $H \to \gamma\gamma$, $H \to ZZ^{(*)} \to 4\ell$, $H \to WW^{(*)} \to \ell\nu\ell\nu$ and $H \to \tau^+\tau^-$, this study has considered low rate Higgs boson channels: VH and $t\bar{t}H$ production with $H \to \gamma\gamma$ decays, and $H \to \mu\mu$. The expected precision on the signal strength precision achieved in each individual channel is shown in Figure 6 (left) for a Higgs boson mass of 125 GeV and integrated luminosities of 300 or 3000 fb^{-1} collected at $\sqrt{s} = 14$ TeV.

Individual measurements are used in a combined statistical analysis. For generality, no assumptions are made on the presence of physics beyond the SM. This means that no assumption can be made on the total width of the Higgs boson, Γ_H, and only ratios of partial widths can be determined. For all production (i) and decay (f) modes, the cross sections times branching ratios, $\sigma_i \times BR_f$, are assumed to be proportional to the product of partial widths given by $\Gamma_i \times \Gamma_f/\Gamma_H$. In the notation of section 2 this means $\Gamma_X/\Gamma_Y = \kappa_X^2/\kappa_Y^2 = \lambda_{XY}^2$, and the relative uncertainty on the ratio is given by $\frac{\Delta(\Gamma_X/\Gamma_Y)}{\Gamma_X/\Gamma_Y} \approx 2 \times \frac{\Delta(\lambda_{XY})}{\lambda_{XY}}$. Figure 6 (right) shows the expected relative uncertainties on the estimated partial width ratios. A minimal coupling benchmark scenario, already discussed in section 2, assumes no new physics and only two independent parameters for the vector (κ_V) and fermion (κ_F) couplings. In this case, experimental precisions of ≈2% on κ_V and ≈3.5% on κ_F are expected with 3000 fb^{-1}.

In order to completely determine the parameters of the SM and establish the Higgs mechanism as the origin of electroweak symmetry breaking, it is important to measure the self-couplings of the Higgs boson. The observation of Higgs boson pair production provides sensitivity to the Higgs trilinear coupling and may be accessible at the LHC. For a Higgs boson mass of around 125 GeV, a relative uncertainty of ≈30% on the Higgs trilinear coupling scale factor should be achievable from observations in the $HH \to b\bar{b}\gamma\gamma$ and $HH \to b\bar{b}\tau^+\tau^-$ channels, assuming 3000 fb^{-1} of $\sqrt{s} = 14$ TeV data.

7. Conclusions

The discovery of a new, Higgs-like boson raises crucial questions on the nature of the new particle, and determines a programme of measurements needed to measure its properties. This paper gives an overview of the latest Higgs studies in ATLAS. After describing the methods used, and results of a first exploration of the couplings of the new particle, it gives a brief description of new searches in the $H \to WW^{(*)} \to \ell\nu\ell\nu$, $H \to \tau^+\tau^-$, and $H \to b\bar{b}$ channels. Finally it gives an overview of the sensitivity achievable in future Higgs boson studies in ATLAS.

References

[1] ATLAS Collaboration, Phys. Lett. **B716**, 1-29 (2012).
[2] CMS Collaboration, Phys. Lett. **B716**, 30-61 (2012).
[3] ATLAS Collaboration, JINST **3** (2008) S08003.
[4] L.D. Landau, Sov. Phys. Doklady **60**, 207 (1948); C.N. Yang, Phys. Rev.**77**, 242 (1950).
[5] ATLAS Collaboration, ATLAS-CONF-2012-127, https://cds.cern.ch/record/1476765.
[6] LHC Higgs Cross-section Working Group, arXiv:1209.0040 [hep-ph].
[7] G. Cowan et al., Eur. Phys. J. C, **71** (2011) 1554; arXiv:1007.1727v2 [physics.data-an].
[8] ATLAS Collaboration, ATLAS-CONF-2012-162, https://cds.cern.ch/record/1494183.
[9] ATLAS Collaboration, ATLAS-CONF-2012-158, https://cds.cern.ch/record/1493601.
[10] LHC Higgs Cross Section Working Group, S. Dittmaier, C. Mariotti, G. Passarino and R. Tanaka Eds., CERN-2011-002, arXiv:hep-ph/1101.0593, CERN, Geneva, 2011.
[11] M. Cacciari,, G.P. Salam, and G.Soyez, JHEP **0804** (2008) 063, `arXiv:0802.1189 [hep-ex]`.
[12] ATLAS Collaboration, ATLAS-CONF-2012-160, https://cds.cern.ch/record/1493624.
[13] A. L. Read, J. Phys. G **28** (2002) 2693.
[14] A. Elagin, P. Murat, A. Pranko and A. Safonov, Nucl. Instr. and Meth. **A654** (2011) 481.
[15] ATLAS Collaboration, ATLAS-CONF-2012-135, https://cds.cern.ch/record/1478423.
[16] ATLAS Collaboration, ATLAS-CONF-2012-161, https://cdsweb.cern.ch/record/1493625/.
[17] ATLAS Collaboration, Phys. Lett. **B718**, 369-390 (2012).
[18] ATLAS Collaboration, ATL-PHYS-PUB-2012-004, https://cdsweb.cern.ch/record/1484890/.